

Identification of Location and Kinetically Defined Mechanism of Cofactors and Reporter Genes in the Cascade of Steroid-regulated Transactivation^{*[5]}

Received for publication, August 29, 2012, and in revised form, October 9, 2012. Published, JBC Papers in Press, October 10, 2012, DOI 10.1074/jbc.M112.414805

John A. Blackford, Jr.[‡], Chunhua Guo[‡], Rong Zhu^{‡1}, Edward J. Dougherty^{‡2}, Carson C. Chow[§], and S. Stoney Simons, Jr.^{‡3}

From the [‡]Steroid Hormones Section, Laboratory of Endocrinology and Receptor Biology and [§]Laboratory of Biological Modeling, NIDDK, National Institutes of Health, Bethesda, Maryland 20892

Background: Current descriptions of steroid hormone action are largely phenomenological rather than mechanistic.

Results: Methodology is described for determining kinetically defined mechanisms and relative sites of action of any two cofactors with steroid receptors.

Conclusion: Position and mode of reporter gene action are constant.

Significance: Location and mechanistic action of cofactors, relative to each other and reporter, is assignable in sequence for receptor-regulated gene transactivation.

A currently obscure area of steroid hormone action is where the component factors, including receptor and reporter gene, act. The DNA binding of factors can be precisely defined, but the location and timing of factor binding and action are usually not equivalent. These questions are addressed for several factors (e.g. glucocorticoid receptor (GR), reporter, TIF2, NCoR, NELF-A, sSMRT, and STAMP) using our recently developed competition assay. This assay reveals both the kinetically defined mechanism of factor action and where the above factors act relative to both each other and the equilibrium equivalent to the rate-limiting step, which we call the concentration limiting step (CLS). The utility of this competition assay would be greatly increased if the position of the CLS is invariant and if the factor acting at the CLS is known. Here we report that the exogenous GREtkLUC reporter acts at the CLS as an accelerator for gene induction by GRs in U2OS cells. This mechanism of reporter function at the CLS persists with different reporters, factors, receptors, and cell types. We, therefore, propose that the reporter gene always acts at the CLS during gene induction and constitutes a landmark around which one can order the actions of all other factors. Current data suggest that how and where GR and the short form of SMRT act is also constant. These results validate a novel and rational methodology for identifying distally acting factors that would be attractive targets for pharmaceutical intervention in the treatment of diseases involving GR-regulated genes.

Most of the steps in steroid-regulated gene transcription are still uncharacterized. For those steps that have been identified, the molecular details generally remain poorly defined. What mechanistic information is available is based almost exclusively upon binding experiments. Thus, the current model for the classical steroid receptors for androgens, estrogens, glucocorticoids, mineralocorticoids, and progestins is that the steroid binds to its cognate receptor in the cytoplasm of cells, the receptor-steroid complex concentrates in the nucleus and binds to DNA and DNA-associated proteins, and a wide variety of cofactors are recruited to the DNA-associated receptor-steroid complexes to regulate gene transcription (1–4).

More than 300 factors have been reported to participate in steroid-regulated gene transactivation (5). However, most factors are described in terms of their effects on the production of monitored product so that very little is known about how any factor acts either kinetically or biochemically. Similarly, where any factor acts is based almost exclusively on where it binds, which is commonly at the promoter region of the transcribed gene. Here, we utilize a recently developed theoretical model of steroid-mediated gene induction (6, 7) to elucidate the properties of factors in steroid hormone action other than factor binding. The theory predicts how the addition of factors will affect the maximal activity (A_{\max}) and the dose-response curve of induced effect *versus* inducer, such as steroid. The dose-response curve is a measure of ligand potency and visually displays the concentration of ligand required for half-maximal activity (EC_{50}). The theory pertains to any process for which the dose-response curve is always a first-order Hill plot. When applied to a competition assay in which the ability of varying concentrations of two factors are simultaneously examined for their ability to alter the A_{\max} and/or EC_{50} , the theory determines both where in the sequence of events each factor acts and the kinetic description of that factor action. These conclusions can be extracted simply by analyzing the properties of various graphs of A_{\max} and EC_{50} as opposed to laborious direct fittings of the data (8). The mechanism of factor action is defined, as in

* This work was supported, in whole or in part, by the Intramural Research Program of the NIDDK, National Institutes of Health.

[5] This article contains supplemental Figs. S1–S7.

¹ Present address: Dept. of Pathology, Shanghai Medical College, Fudan University, 200032 Shanghai, China.

² Present address: Bldg. 10, Rm. 4D06, Warren Grant Magnuson Clinical Center, National Institutes of Health, Bethesda, MD 20892-1662.

³ To whom correspondence should be addressed: Bldg. 10, Rm. 8N-307B, NIDDK/CEB, NIH, Bethesda, MD 20892-1772. Tel.: 301-496-6796; Fax: 301-402-3572; E-mail: stoney@helix.nih.gov.

enzyme kinetics, by its kinetic properties, which can be unambiguously described as that of an “activator” (or accelerator) or as one of six types of “inhibitors” (or decelerators: competitive, uncompetitive, non-competitive, linear, partial, and mixed). These definitions refer specifically to the action of the factor on a specific step or reaction that is embedded in a sequence of other reactions. These terms should not be confused with the empirically derived classifications of “coactivators” and “corepressors,” which do not convey any mechanistic insight.

It is well known from enzyme kinetics that an inhibitor can actually cause an increase in total response if the inhibitor blocks a high frequency but low efficiency pathway and thus diverts the reaction scheme to a lower frequency but higher efficiency step (6, 9, 10). Conversely, an activator can lead to decreased gene expression. Such contrary actions, which defy simple categorization based on the observed levels of gene expression, may explain reports of single factors having opposite effects on different inducible genes in the same cell (11–13). This dilemma can theoretically be resolved by our competition assay, which examines not only the A_{\max} but also the EC_{50} in the analysis of gene induction. When both parameters of gene induction are quantitated and graphed in manners other than the conventional A_{\max} versus factor, it is possible to define the kinetic mechanism of action of the two competing factors in that assay system (8).

Another major difference with the many widely employed binding assays, including the very powerful ChIP-Seq assays, is that our competition assay identifies where a factor acts, as opposed to binds, in the multistep process of gene induction. It is common knowledge that when and where a factor binds is often unrelated to factor action. The number of binding sites in the genome for the glucocorticoid receptor (GR)⁴ is ~10-fold greater than the number of induced genes (14, 15). p300 is recruited by added androgen to the androgen-responsive elements of the *TMPRSS2* and *FKBP5* genes but is required for androgen induction of only the former gene (13). RNA polymerase II is frequently found bound to pausing sites at about 50 bp downstream from the start of transcription of the induced gene but is not engaged in elongation until a later time (16–18). Histone acetyltransferases are recruited to glucocorticoid response elements (GREs) by GR-steroid complexes to acetylate histones in a manner that is thought to facilitate gene activation (19). However, these acetylated histones almost certainly do not directly affect gene transcription. The histone marks for GR-inducible genes in human A549 lung cancer cells are found to exist before the addition of the glucocorticoid agonist dexamethasone (Dex) (20). Conversely, activation of class I transcription by γ interferon (or its inhibition by α -amanitin) does not alter histone modifications in any of the tissues examined (21). Thus, not only is it difficult to determine factor activity from the occurrence of factor binding but also it appears that a factor/cofactor actually influences gene transcription at a step downstream of its binding.

⁴ The abbreviations used are: GR, glucocorticoid receptor; GRE, glucocorticoid response element; Dex, dexamethasone; CLS, concentration limiting step; CBP, CREB (cAMP response element-binding protein) binding protein; PR, progesterone receptor; tk, thymidine kinase.

Information about where a factor acts, as opposed to binds, is readily determined from our competition assay using simple graphical analyses of A_{\max} and EC_{50} (8). These graphs supplant the usual A_{\max} versus factor that populate the literature. Instead, we plot $1/EC_{50}$, A_{\max}/EC_{50} , and EC_{50}/A_{\max} versus factor. These graphs, although unconventional, are unique in being able to determine where two factors work relative to each other and to the steady state equivalent of the rate-limiting step, which is called the concentration limiting step (CLS). The CLS is that step after which the concentration of the bound factors is much less than the free concentration and is analogous, but not equivalent to, the rate-limiting step in enzyme kinetics (6, 8). An important difference between the CLS of equilibrium systems and the rate-limiting step of enzyme kinetics is that although a factor present at low concentrations is a candidate for acting at the CLS, that factor does not have to act at the CLS.

The utility of the competition assay has been illustrated in the assignment of kinetic action, and site of action relative to the CLS, for the coactivator TIF2 and the corepressor sSMRT during GR-regulated transactivation of both exogenous and endogenous genes (8). However, as more factors known to modulate the A_{\max} and EC_{50} of steroid receptors (22, 23) are analyzed by this method, the critical question arises of whether the location of the CLS is fixed or changes with the composition of the added factors. With all of the species described so far that can contribute to receptor-steroid control of gene expression (5), there is no *a priori* reason to believe that the site of any factor action, including the CLS, would be immovable under all conditions. Conversely, if the position of the CLS is constant, this would make the CLS an invaluable standard reference point about which one could use overlapping competition assays to order the actions of all other factors.

The purpose of this study is to examine whether the CLS changes or remains constant under different conditions. We find that synthetic reporters act at the CLS under 12 different conditions. Further studies with GR and the corepressor sSMRT show that the action and positioning in the sequence of reactions for gene induction of each factor also appears to be constant. These results argue that the CLS and the actions of at least two factors (GR and sSMRT) are invariant under the examined conditions and have been used as markers while constructing a sequence of actions of 10 other factors under assorted conditions. This sequence of actions will be invaluable in constructing a broader mechanism of steroid hormone action and will facilitate identifying factors acting close to the final response. Such factors would be attractive targets for pharmacological intervention because the number of side effects would be expected to be fewer than when altering a step closer to the beginning of the overall sequence of events.

EXPERIMENTAL PROCEDURES

Unless otherwise indicated, all cell growth was at 37 °C, and all other operations were performed at room temperature.

Chemicals—Dex was purchased from Sigma. Restriction enzymes and T4 DNA ligase were from New England Biolabs (Beverly, MA), and the dual-luciferase reporter assay was from Promega (Madison, WI).

Factor and Reporter Mechanisms in Steroid Hormone Action

Plasmids—Renilla-TS reporter and GREtkLUC have been previously described (24). FR-LUC reporter is from Stratagene (La Jolla, CA). pCMX/sSMRT was a gift from Ronald Evans (Salk Institute, La Jolla, CA), NCoR/FLAG was from Geoff Rosenfeld (University of California-San Diego, San Diego, CA), NELF-A (25) and FLAG/NELF-B (containing the 52 C-terminal residues of the neomycin resistance protein in place of the C-terminal 30 amino acids of NELF-B) were from Rong Li (University of Texas Health Science Center at San Antonio), pCDNA3.1+/mCBP.HA was from Janardan K. Reddy (Feinberg School of Medicine, Northwestern University, Chicago, IL), and MMTVLuc (pLTRLUC) was from Gordon Hager (NCI/National Institutes of Health). pSG5/rat GR, pSG5/human serum albumin, pCMX/human serum albumin, and pBSK have been previously described (26–29).⁵ GREtkGFP was prepared by first using Fast Start PCR Master Mix (Roche Applied Science, 12-140-314-001, Indianapolis, IN) and the primers 5'-CGGCCCCGGGCTAGAACATCCTGTACAGGATCCG-TAG-3' and 5'-CGGACCGGTACCAACAGTACCGGAATGCCAAGCTTCG-3' to introduce, respectively, a SmaI site 5' of, and an AgeI site 3' of the GREtk sequences at bp 437–684 of GREtkLUC. PCR was performed at 95 °C for 4 min, then 30 cycles of 95 °C for 30 s plus 65 °C for 30 s and 73 °C for 30 s, then 72 °C for 7 min, and held at 4 °C. The PCR product was confirmed on a 2% agarose gel and purified with a Qiaquick gel extraction kit (Qiagen, 28704, Valencia, CA). The PCR product and promoterless vector pAcGFP1–1 (Clontech, 632497, Mountain View, CA) were sequentially digested with AgeI (Fermentas, FD1464, Glen Burnie, MD) and SmaI (Fermentas, FD0664) at 37 °C for 1 h each. The vector was purified with a QIAprep spin miniprep kit (Qiagen, 27104). The PCR product was purified with a Qiaquick gel extraction kit (Qiagen, 28704). The digested and purified PCR product and vector were ligated with T4 DNA ligase (Fermentas, EL0014) at 16 °C overnight and then transformed into subcloning efficiency DH5 α (Invitrogen, 18265-017). Clones were confirmed by sequencing. GRE-GFP Dex-dependent expression was confirmed by fluorescent microscopy and quantitative real-time PCR with the primers AcGFP (5'-TTGCCATCCTCCTTGAAATC) and AcGFP (3'-CACATGAAGCAGCAGCACTT).

Antibodies and Western Blotting—Anti-GR mouse and rabbit monoclonal antibodies (MA1–510 and PA1–516A; Affinity BioReagents), anti-NELF-A rabbit polyclonal antibody (32911; Santa Cruz, Santa Cruz, CA), anti-CBP rabbit polyclonal antibody (ab2832; Abcam, Cambridge, MA), anti- β actin mouse monoclonal antibody (A2228; Sigma), anti-SMRT and anti-PR-B rabbit antibodies (06-891 and 04-1018, respectively; Millipore, Billerica, MA), and anti-FLAG mouse monoclonal antibody (F3165; Sigma) are commercially available. Anti-NCoR rabbit antibody was a gift from Dr. Geoff Rosenfeld (University of California-San Diego). Anti-STAMP antibody has been previously described (30). Western blots were prepared, probed with the appropriate antibodies, and visualized by ECL detection reagents as described by the manufacturer (Amersham Biosciences).

Cell Culture, Transient Transfection, and Reporter Analysis—Monolayer cultures of U2OS, CV-1, 293, and 1470.2 cells were grown as described previously (8, 30–32). Triplicate samples of cells were seeded into 24-well plates at 20,000–30,000 cells per well and transiently transfected the following day with luciferase reporter and DNA plasmids by using 0.7 μ l of Lipofectamine (Invitrogen) or FuGENE 6 (Roche Applied Science) per well according to the manufacturer's instructions. The total transfected DNA was adjusted to 300 ng/well of a 24-well plate with pBluescriptII SK+ (Stratagene). The molar amount of plasmids expressing different protein constructs was kept constant with added empty plasmid or plasmid expressing human serum albumin (24). Renilla-TS (10 ng/well of a 24-well plate) was included as an internal control. After transfection (28–32 h), cells were treated with medium containing appropriate hormone dilutions. The cells were lysed 16–20 h later and assayed for reporter gene activity using dual luciferase assay reagents according to the manufacturer's instructions (Promega). Luciferase activity was measured by an EG&G Berthold's luminometer (Microumat LB 96P) or a GloMax[®] 96 Microplate Luminometer (Promega). The data were normalized to Renilla TS luciferase activity and expressed as a percentage of the maximal response with Dex before being plotted \pm S.E. unless otherwise noted.

Two-factor Competition Assays—A full description is to be found elsewhere (8). When different amounts of plasmid encoding a protein are transfected, the total molar amount of vector DNA is kept constant with the addition of the required amount of empty vector. However, when the Luciferase reporter plasmid is varied, no balancing plasmid (such as LUC to balance GREtkLUC) is usually added because the low background activity of LUC is often enough to distort the graphs of A_{\max}/EC_{50} versus reporter. This practice does not introduce any artifactual results, as verified by graphs of A_{\max} versus ng of reporter plasmid giving the expected linear plots that go through the origin (data not shown). Briefly, the rest of the assay proceeds as follows. The luciferase activity in each treatment is determined on an EG&G Berthold's luminometer (Microumat LB 96P) or a GloMax[®] 96 Microplate Luminometer. The maximum induced activity (A_{\max}) and EC_{50} are obtained from directly fitting a Michaelis-Menten curve to the average ($n = 3$) value of induced luciferase activity at three concentrations of Dex (the middle concentration being near the EC_{50}) plus a vehicle (EtOH) control. Graphs of $1/EC_{50}$ and A_{\max}/EC_{50} versus the concentration of one cofactor were constructed at each of the concentrations of the second factor. Western blots often reveal a nonlinear relationship between the optical density of scanned protein band and the amount of transfected plasmid at constant levels either of total cellular protein or of an internal standard such as β -actin. To determine the linear equivalent of expressed plasmid, the nonlinear plot of absorbance versus ng of transfected plasmid is first fit to a Michaelis-Menten plot of

$$A_{\max} = m1 \times \text{plasmid}/(m2 + \text{plasmid}) \quad (\text{Eq. 1})$$

The functional equivalent of the transfected plasmid that gives a linear absorbance versus plasmid plot is then obtained from the formula of

⁵ Z. Zhang, Y. Sun, Y.-W. Cho, C. C. Chow, and S. S. Simons, Jr., submitted for publication.

$$\text{Plasmid}(\text{linear}) = m_2 \times \text{plasmid} / (m_2 + \text{plasmid}) \quad (\text{Eq. 2})$$

The x axis value of amount of plasmid in the various graphs is then this “corrected plasmid” value. If an experiment used n concentrations for each cofactor, then there would be a total of four graphs, each with n separate curves. The shape of the curves and how they change with the other cofactor are then compared with Table S1 in Dougherty *et al.* (8) to determine the mechanism and order of action.

Many of the entries in Table S1 of Ref. 8 require an estimate of the intersection point of a set of linear regression fits to the graphs. For a family of lines of the form $y = a_i + b_i x$, an unbiased estimate of the intersection can be obtained from a linear regression on the graph of a versus b to give a new plot of the form $a = y' - x' b$, where y' is the y axis value of the intersection point of the family of lines in the original graph, and x' (negative of the regression coefficient) corresponds to the x axis value of the intersection point.

Statistical Analysis—Unless otherwise noted, all experiments were performed in triplicate multiple times. Kaleida-Graph 4.1 (Synergy Software, Reading, PA) was used to determine a least-squares best fit (R^2 was almost always >0.95) of the experimental data to the theoretical dose-response curve, which is given by the equation derived from Michaelis-Menten kinetics of $y = (\text{free steroid}) / (\text{free steroid} + \text{distribution constant } (K_d))$ (where the concentration of total steroid is approximately equal to the concentration of free steroid because only a small portion is bound) to yield a single EC_{50} value. The values of n independent experiments were then analyzed for statistical significance by the two-tailed Student's t test using InStat 2.03 for Macintosh (GraphPad Software, San Diego, CA). When the difference between the S.D. values of two populations was significantly different, then the Mann-Whitney test or the Alternate Welch t test was used.

RESULTS

Terminology of Assays—The labels coactivators and corepressors are widely used for cofactors in the current hormone action literature. These definitions are based solely on how the cofactor affects the observed response. However, gene induction is a process that consists of a sequence of many steps or “reactions,” and thus the local action of a coactivator or corepressor on its specific reaction could be either activating or inhibiting. For example, a classically defined coactivator could increase the total response by inhibiting another inhibitor or activating another activator. Hence, to disambiguate the local action from the global action, we use the term activator or accelerator for a factor that increases the output of the local reaction independent of the observed final response (*e.g.* amount of gene product). Similarly, we use inhibitor or decelerator for a factor that decreases the output of a local reaction. As previously reported (6–8), a cofactor can be either an accelerator or one of six types of decelerators: competitive, uncompetitive, noncompetitive, linear, partial, and mixed.

Candidate Factors Acting at the CLS—The theory for steroid-regulated gene induction consists of a sequence of reac-

tions involving accelerators that can be acted upon by decelerators. We seek the identity of the accelerator that acts at the CLS and any decelerators that act upon it. This involves an application of the graphical method to experimental data as described below. According to the theory, we can also restrict our search for accelerators acting at the CLS to essential factors, which are species that when absent reduce the observed response to zero (6–8). There are, unfortunately, no simple ways to prescreen for decelerators. Given the numerous pivotal factors (*e.g.* steroid, receptor, reporter, RNA polymerase II, etc.) in the current model of steroid hormone action (2–4) plus the kinetic restriction that two accelerators cannot act at the same step, it is a non-trivial issue of identifying which factor is functioning at the CLS.

The first two candidates considered were 1) CBP, which binds to p160 coactivators that are associated with DNA-bound GRs and has been proposed to act as a platform for the assembly of other cofactors (33), and 2) the induced gene itself, which is where most of the factors initially congregate. This latter possibility dictated that the experiments be conducted with transiently transfected reporter genes. This is because the competition assays require using changing concentrations of the factor being investigated (8). It is much easier and more controllable to vary the amounts of target gene added to transiently transfected cells than to generate cells containing different amounts of an endogenous target gene. We chose to employ two different reporter genes: GREtkLUC and MMTVLuc. GREtkLUC contains an inverted tandem repeat of the second GRE of the rat tyrosine aminotransferase gene upstream of the tk promoter to regulate the luciferase gene (34). MMTVLuc consists of the mouse mammary tumor virus upstream enhancer, containing several GREs, and promoter region (35), driving the luciferase reporter. Our experimental system utilizes transiently transfected U2OS cells, which contain very low levels of GR and with which we have considerable experience (7, 8, 36, 37).

A prerequisite for using our theory to analyze different assay combinations is that the dose-response curve for the production of the final product follows a first-order Hill plot in which the response goes from 10 to 90% of maximum over an 81-fold range of steroid concentration (6). As shown in Fig. 1, A and B, for two concentrations of GREtkLUC, and in Fig. 1C, for a single high concentration of MMTVLuc, the dose-response curves for both reporters satisfy the requirements of a first-order Hill plot. Thus, these induction systems can be used in our competition assay.

Another prerequisite of the competition assay is that the two factors to be examined must influence either the A_{max} or the EC_{50} of the induction reaction. The data of Fig. 1D confirm that in the present system both CBP and sSMRT alter the A_{max} of induced luciferase activity. sSMRT is the short form of the corepressor SMRT (38) and lacks about 1000 N-terminal residues (39) but is still an active corepressor, as seen in Fig. 1D. Similarly, different concentrations of GR and both GREtkLUC (Fig. 1E) and MMTVLuc (data not shown) affect the A_{max} . Thus, all of the requirements for using sSMRT versus CBP and GR versus GREtkLUC or MMTVLuc in our competition assay have been met.

Factor and Reporter Mechanisms in Steroid Hormone Action

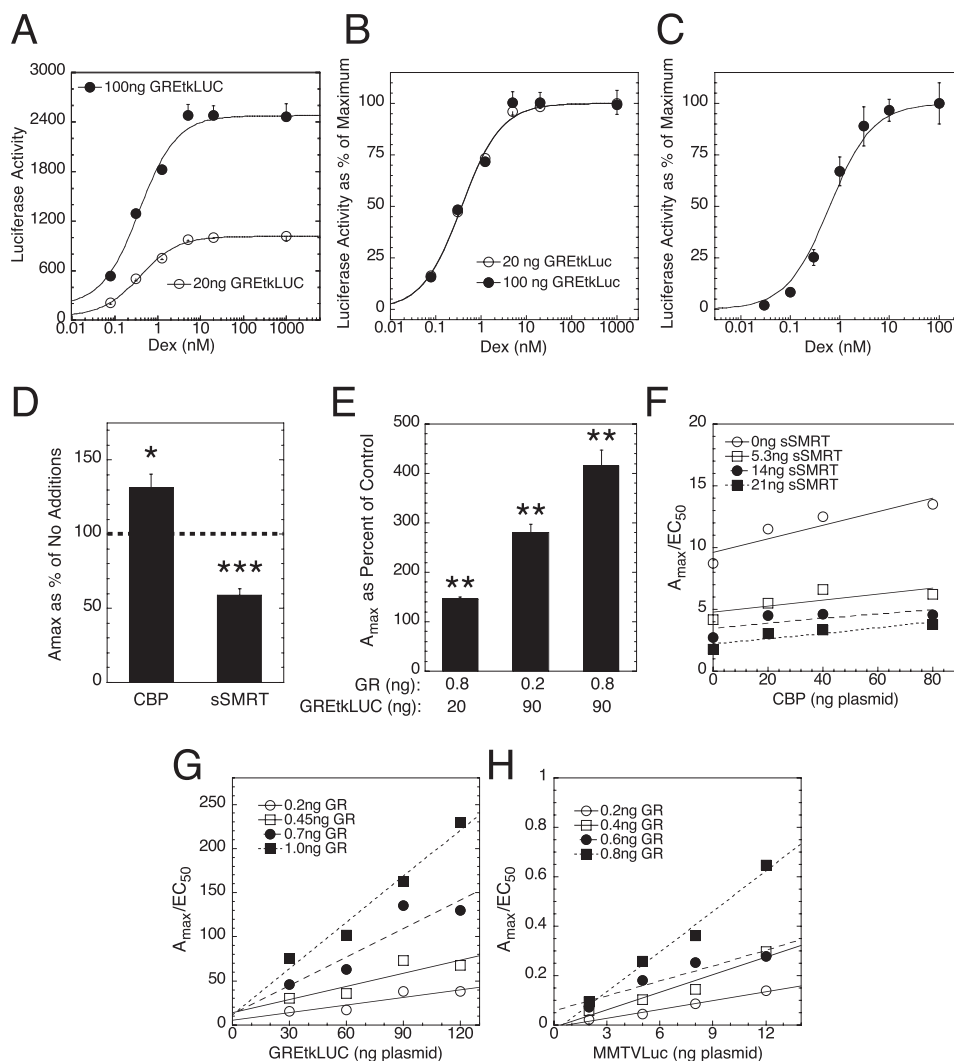


FIGURE 1. Characteristics of the competition assay in U2OS cells. *A* and *B*, dose-response curves for GR induction of exogenous GREtkLUC reporter give first-order Hill plots of different amplitudes. GR (0.5 ng of plasmid) induction of two amounts of transiently transfected GREtkLUC plasmid with different concentrations of Dex was conducted, and the results of a single representative experiment were then plotted, as described under "Experimental Procedures." The effect of varying reporter on the A_{max} is displayed in *A*, whereas the influence of reporter concentration on the EC_{50} is given in *B*. *C*, a dose-response curve for GR induction of exogenous MMTVLuc reporter is first order. U2OS cells were transiently transfected with GR (0.8 ng) and MMTVLuc (100 ng) and treated with Dex, and the results of a single representative experiment are plotted as in *B*. *D*, CBP increases, and sSMRT decreases GR induction of GREtkLUC. U2OS cells were transiently transfected with GR (0.5 ng) and GREtkLUC (100 ng) plus 80 ng of CBP plasmid or 40 ng of sSMRT and induced by three subsaturating concentrations of Dex. In all instances an empty vector(s) was added to maintain a constant molar equivalent of the vector for the sSMRT and CBP plasmids. Luciferase activity was determined, and the A_{max} at saturating Dex concentrations was determined by exact curve fitting as described under "Experimental Procedures." The A_{max} with CBP and sSMRT was expressed as percent of that for cells with no added factor, and the average value (\pm S.E.) from six independent experiments was plotted. The *dashed line* indicates no change relative to cells with no addition. *, $p < 0.02$; ***, $p < 0.0003$ compared with no addition. *E*, the ability of GR and GREtkLUC to increase A_{max} is additive. Cells were transfected with 0.2 ng of GR and 20 ng of GREtkLUC plasmids (control cells) or the indicated amounts of GR and GREtkLUC and induced with subsaturating Dex concentrations before graphically determining the A_{max} for induced luciferase at saturating Dex as described in *panel D*. The A_{max} for each composition of GR and GREtkLUC was expressed as percent of control cells. The average values (\pm S.E.) from four independent experiments were then plotted. **, $p \leq 0.002$ compared with control cells. *F-H*, different graphical properties of the common plot of A_{max}/EC_{50} versus factor are shown. All combinations of four concentrations each of CBP and sSMRT plasmid (plus 5 ng of GR and 100 ng of GREtkLUC) or the indicated amounts of GR and GREtkLUC or MMTVLuc for a total of 16 sets were used to cotransfect U2OS cells, which were then treated with three subsaturating concentrations of Dex before determining the amounts of induced luciferase. Exact fits of these data to a first-order Hill plot yielded the A_{max} and EC_{50} for each combination as described under "Experimental Procedures." Graphs of A_{max}/EC_{50} versus CBP (*F*), versus GREtkLUC (*G*), and versus MMTVLuc (*H*) at different concentrations of the other factor were constructed and analyzed as detailed under "Results." Graphs shown are for a single representative experiment (total = 3–5).

The competition assays are conducted by transfecting cells with all combinations of four concentrations of the two competing factors. Constant amounts of receptor and/or reporter are also added if they are not one of the competing factors. The transfected cells are then induced with triplicate samples of three subsaturating concentrations of an agonist steroid: Dex for GR and R5020 for progesterone receptor (PR). Induction curves are best fit to the experimental data as described under

"Experimental Procedures" to yield the A_{max} and EC_{50} for all of the 16 combinations of the two factors. Two to three sets of graphs are then constructed ($1/EC_{50}$ and A_{max}/EC_{50} , plus EC_{50}/A_{max} when encountering a decelerator) versus Factor 1 with the four different concentrations of Factor 2 (and *vice versa*). The graphs of A_{max}/EC_{50} are particularly diagnostic of similar *versus* different modes and sites of action. This is because both components (A_{max} and EC_{50}) can be modulated by a variety of

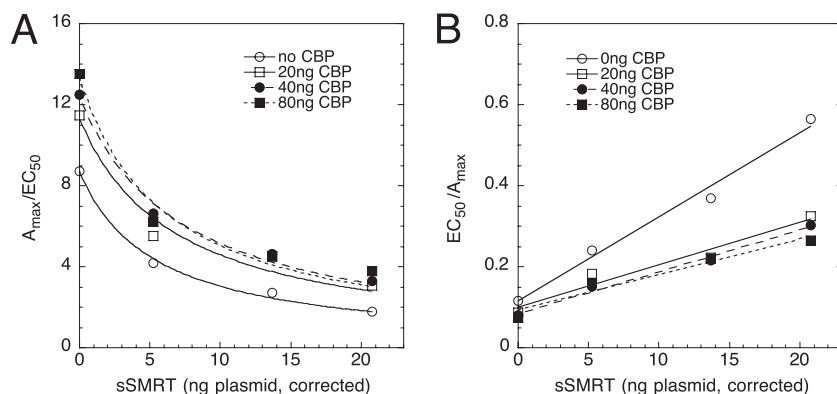


FIGURE 2. **Competition assay for CBP and sSMRT during GR-mediated induction in U2OS cells.** Assays were conducted as described for Fig. 1F. Graphs of A_{\max}/EC_{50} versus sSMRT (A), and EC_{50}/A_{\max} versus sSMRT (B) at different concentrations of the other factor, CBP, were constructed and analyzed as detailed under "Results." Graphs shown are for a single representative experiment (total = 5).

factors (22, 23), thereby reducing the possibility that factors with dissimilar actions will yield graphs with the same characteristics, such as slope (positive or negative and linear or curvilinear), change in the position of each curve described for increasing first factor at each concentration of the second factor, and position of the intersection point of the four sets of curves in each plot.

In all plots the amount of transfected plasmid on the abscissa assumes that the expression of protein increases linearly. Western blots are run to determine the expression efficiency from increasing amounts of plasmid. If the expression is not linear but falls off with increasing plasmid, then the added amounts of plasmid are corrected as described under "Experimental Procedures" to reflect the lower levels of transfected plasmid that would have been used if the expression had been linear.

The first three competition assays run of factors that might act at the CLS involved varying the amounts of CBP, GREtkLUC, and MMTVLuc with sSMRT or GR as competitor. Western blots revealed that the expression level of transfected CBP and GR was linear in the range of plasmids used (data not shown) so that no correction is needed. With sSMRT, the expression is nonlinear over the range of 0–40 ng of plasmid and has been corrected as described under "Experimental Procedures" (data not shown). The graph of A_{\max}/EC_{50} versus CBP with increasing sSMRT competitor (Fig. 1F) has very different characteristics from those of A_{\max}/EC_{50} versus GREtkLUC or MMTVLuc with added GR (Fig. 1, G and H, respectively). Although all three plots are linear with positive slopes, the position of the lines decreases with higher levels of sSMRT (the competitor of CBP) (Fig. 1F) but increases with the competitor (GR) of GREtkLUC (Fig. 1G) and MMTVLuc (Fig. 1H). Also, the lines in Fig. 1F appear to intersect at a large negative value of CBP plasmid, whereas the intersection points in Fig. 1, G and H, both are essentially at the origin. The almost identical properties of GR competition with GREtkLUC or MMTVLuc compared with sSMRT competition with CBP strongly suggest that the actions of GR with GREtkLUC and MMTVLuc are the same, in which case GREtkLUC and MMTVLuc would have the same action at the same location of the overall scheme of gene induction. To determine the precise nature of GREtkLUC and

MMTVLuc activity, we applied the full analytical features of the competition assay (8) as described below.

Procedure for Analysis of Competition Assays—As mentioned above, each competition assay generates 2–3 sets of graphs ($1/EC_{50}$ and A_{\max}/EC_{50} , plus EC_{50}/A_{\max} when encountering a decelerator) versus Factor 1 with the four different concentrations of Factor 2 (and *vice versa*) for a total of 4–6 graphs. The characteristics of each graph (*i.e.* shape and slope of the curves, effect of the second factor on the position of the curves plotted against the first factor, location of the intersection point of the curves, and the value of the y axis intercept of each curve) were then matched with the possible scenarios listed in the supplemental Table S1 in Dougherty *et al.* (8). Each graphical scenario is associated with one or more distinct mechanistic explanations. This table encompasses >74% of the possible theoretical mechanistic combinations and has covered all of the experimentally observed graphical behaviors observed to date (6–8, 23). When the S.D. of the experimental triplicates of the induction curves are $\leq 10\%$, the total of four to six graphs can uniquely implicate a single mechanistic explanation both for the kinetically defined mechanism of action of each factor and for the ordering of the actions of the two factors relative to the CLS and often relative to each other.

It should be stressed that more than one mechanistic explanation is usually associated with the shape of each graph in Table S1 of Ref. 8. Furthermore, given the inherent inaccuracies of biological experiments, the observed graphs may adequately fit the description of more than one graph in Table S1 (8). Nevertheless, the requirement that one of the possible descriptions be the same (or mechanistically inclusive) in each of the four to six graphs severely limits the available explanatory options. Thus, the ability of this graphical analysis to yield agreement on a single mechanistic explanation is extremely significant and strongly supports the accuracy of the conclusion even with normal experimental errors.

CBP Does Not Act at the CLS—To gain more information about the kinetic mechanism of CBP (and sSMRT) action and where each factor acts, we consider the diagnostic plots of A_{\max}/EC_{50} versus sSMRT (Fig. 2A) and EC_{50}/A_{\max} versus sSMRT (Fig. 2B) in addition to the above A_{\max}/EC_{50} versus CBP (Fig. 1F). The interpretation of A_{\max}/EC_{50} versus CBP (Fig. 1F)

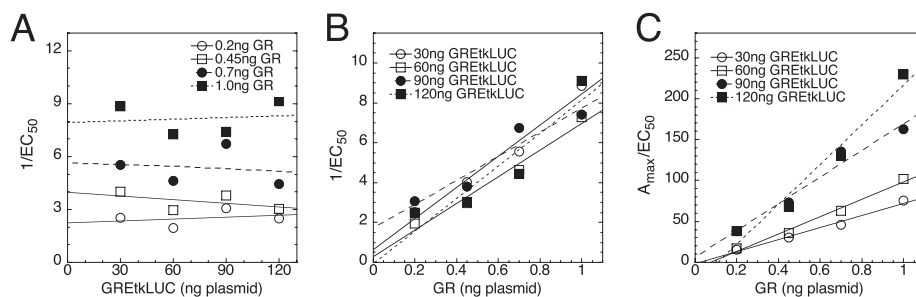


FIGURE 3. **Competition assay with GR and GREtkLUC during GR-mediated induction in U2OS cells.** Assays were conducted as described for Fig. 1F. Graphs of $1/EC_{50}$ versus GREtkLUC (A), $1/EC_{50}$ versus GR (B), and A_{max}/EC_{50} versus GREtkLUC (C) at different concentrations of the other factor were constructed and analyzed as detailed under "Results." Graphs shown are for a single representative experiment (total = 4).

depends upon the coordinates of the intersection point of the four lines relative to the amount of endogenous CBP, which Western blots reveal is equivalent to 2 ng of transfected CBP plasmid (data not shown; see also "Experimental Procedures"). The average intersection values (\pm S.D.) from five experiments like Fig. 1F are $x = -182 \pm 46$ ng of CBP plasmid, and $y = -0.33 \pm 0.41$. These values match with the description in Table S1 (8) of that graph where the intersection point is at $y = 0$, $x <$ endogenous F1 (CBP; *i.e.* -182 versus no endogenous CBP being -2), and y axis intercepts are >0 and decrease with increasing F2 (sSMRT). The mechanism associated with this graph is that CBP (F1) is an accelerator after the CLS, whereas sSMRT (F2) is a competitive or mixed decelerator before or at the CLS and thus before CBP (abbreviated as: $CBP = A > CLS$, $sSMRT = C$ or $M \leq CLS$, $sSMRT < CBP$).

The interpretation of A_{max}/EC_{50} versus sSMRT (Fig. 2A) depends upon whether the decreasing curves plateau at zero or some positive non-zero value with infinite sSMRT. The fact that the inverse plot (EC_{50}/A_{max} versus sSMRT; Fig. 2B) is linear means that the graph of A_{max}/EC_{50} versus sSMRT goes to zero at infinite sSMRT (note that if the plots were to plateau at some finite value y' , then the graph of EC_{50}/A_{max} versus sSMRT would yield plots that curved downward from linear and that this downward curvature would disappear if y' was first subtracted from each value of A_{max}/EC_{50} before plotting the reciprocal). According to the reference table (8), this graphical behavior is due to $CBP = A$ and $sSMRT = C \leq CLS$. The only mechanistic interpretation that is shared by the graphs of A_{max}/EC_{50} versus CBP and versus sSMRT is that $CBP = A > CLS$, $sSMRT = C \leq CLS$, and $sSMRT < CBP$. It should be noted that the plots of $1/EC_{50}$ versus each factor match graphs that have these same mechanistic conclusion as possible interpretations (data not shown). Thus, all of the graphs yield one single, consistent mechanistic conclusion of $CBP = A > CLS$, $sSMRT = C \leq CLS$, and $sSMRT < CBP$. Furthermore, this reveals that CBP does not act at the CLS.

GREtkLUC Acts at the CLS in U2OS Cells—To further characterize the mode and site of action of the reporter in the competition of GR and GREtkLUC, the plots of $1/EC_{50}$ versus GREtkLUC (Fig. 3A) were first examined. They have slopes that are not significantly different from zero. For four experiments using transfected GR plasmids between 0.15 and 0.8 ng, the average of each individual line (corresponding to low, low-medium, high-medium, and high GR plasmid level) is not statistically different from each other, and only the slopes with the lowest amount of

GR were different from zero (data not shown). These results are also consistent with those of Fig. 1, A and B, where the EC_{50} is the same with 20 and 100 ng of GREtkLUC. Thus it is justified to average each of the four slopes in all 4 experiments, which gives a value of 0.0013 ± 0.0019 (S.D., $n = 16$) that is also not statistically different from zero. This behavior coupled with the higher position of each line with increasing GR is associated with several mechanisms, one of which is $GREtkLUC = A = CLS$ and $GR = A \neq CLS$. Graphs of $1/EC_{50}$ versus GR (Fig. 3B) have the average behavior of no reproducible difference between the position and slope of the lines with changing amounts of GREtkLUC. According to the reference table (8), these two graphs of $1/EC_{50}$ restrict the mechanistic interpretations to $GREtkLUC = A = CLS$, and GR is either $A \neq CLS$ or an uncompetitive inhibitor at the CLS.

The graph of A_{max}/EC_{50} versus GR (Fig. 3C) displays an intersection point at the origin (average intersection points: $x = 0.014 \pm 0.13$ ng plasmid, $y = 4.2 \pm 6.1$). It should be noted that Western blots show that the level of endogenous GR is minimal compared with the transfected GR. Thus the true zero on the x axis, where there is no endogenous or exogenous GR, is the current zero. This property limits the options for GR position and type of action to $GR = A < CLS$. The above graph of A_{max}/EC_{50} versus GREtkLUC (Fig. 1G) is also compatible with these conclusions, although the intersection point shows greater variation from an intersection point at the origin ($x = -37 \pm 35$, $y = 2.9 \pm 7.8$). Thus the combined results are consistent with $GREtkLUC = A = CLS$ and $GR = A < CLS$.

MMTVLuc Acts at the CLS in U2OS Cells—The above results show that the reporter, GREtkLUC, functions as an accelerator at the CLS (Fig. 3) and that GREtkLUC and MMTVLuc appear to give nearly identical responses in graphs of A_{max}/EC_{50} versus reporter with varying GR (Fig. 1, G and H). However, it is plausible that the slight alteration of a factor acting as $A = CLS$ under one set of conditions could be replaced by another essential factor or displaced to a position before or after the CLS under different conditions. To answer whether such changes might occur when replacing GREtkLUC with MMTVLuc, we examined the data of the competition assay of Fig. 1H in greater detail. The critical additional graphs are summarized in Table 1 and shown in supplemental Figs. S1. Together, all of the graphs yield the consistent and unique conclusion that $MMTVLuc = A = CLS$ and $GR = A < CLS$. Thus the inducible reporter acts as an accelerator at the CLS irrespective of the nature of the

TABLE 1
Critical graphs from competition assays with GR Induction of reporter genes

The pairs of factors analyzed in competition assays are listed under “factors” (first factor = F1, second factor = F2) and separated by double horizontal lines for different reporters or cell lines (in bold type) and by single horizontal lines for different pairings in the same cell line. The three types of graphs ($1/EC_{50}$, A_{max}/EC_{50} , and EC_{50}/A_{max}) versus each factor are listed at the top, with the characteristics of the most informative graphs versus F1 or versus F2 listed below the relevant factor. In these columns, > and < mean “increases” and “decreases”, respectively. The unique mechanistic conclusion for each pair is listed at the far right under “Mechanism”. In this column, =, <, and \leq mean “at”, “before”, and “before or at”, respectively.

Factors	1/EC ₅₀ vs.		A _{max} /EC ₅₀ vs.		EC ₅₀ /A _{max} vs.		Mechanism	
	F1	F2	F1	F2	F1	F2		
USOS cells with GR and MMTVLuc								
MMTVLuc	slope = 0		lines intersect at origin, slope > with F2	lines intersect at origin, slope > with F1			MMTVLuc is A = CLS, GR is A < CLS	
and GR	(-0.0041 ± 0.011, S.D., n = 12, 3 exper.), y-axis intercept > with F2							
USOS cells with GR and GREtkLUC								
GREtkLUC	slope = 0				linear, slope < with F1	GREtkLUC is A = CLS, GREtkGFP is C \leq CLS		
and GREtkGFP	(-0.00014 ± 0.00055, S.D., n = 20, 5 exper.)							
GREtkLUC	slope = 0		lines intersect at origin, slope < with F2			linear, slope < with F1	GREtkLUC is A = CLS, sSMRT is C \leq CLS	
and sSMRT	(0.00038 ± 0.0013, S.D., n = 12, 3 exper.), y-axis intercept < with F2							
GREtkLUC	slope = 0		lines intersect at origin, slope < with F2			linear, slope < with F1	GREtkLUC is A = CLS, STAMP is C \leq CLS	
and STAMP	(0.0004 ± 0.0012, S.D., n = 16, 4 exper.), y-axis intercept < with F2							
GREtkLUC	slope = 0				plots curve up (see text)	GREtkLUC is A = CLS, NELF-A is C at 2 sites \leq CLS		
and NELF-A	(0.006 ± 0.011, S.D., n = 20, 5 exper.), y-axis intercept < with F2							
GREtkLUC	slope = 0				plots curve up (see text)	GREtkLUC is A = CLS, NELF-B is C at 2 sites \leq CLS		
and NELF-B	(-0.0004 ± 0.00089, S.D., n = 20, 5 exper.), y-axis intercept < with F2							
CV-1 cells with GR and GREtkLUC								
GREtkLUC	slope = 0		lines intersect at origin, slope > with F1			GREtkLUC is A = CLS, GR is A < CLS		
and GR	(-0.0010 ± 0.0061, S.D., n = 12, 3 exper.), y-axis intercept > with F2							
293 cells with GR and GREtkLUC								
GREtkLUC	slope = 0		lines intersect at origin, slope > with F1			GREtkLUC is A = CLS, GR is A < CLS		
and GR	(-0.0015 ± 0.0025, S.D., n = 12, 3 exper.), y-axis intercept > with F2							
1470.2 cells with GR and GREtkLUC								
GREtkLUC	slope = 0				linear, slope < with F1	GREtkLUC is A = CLS, sSMRT is C \leq CLS		
and sSMRT	(0.0000 ± 0.0001, S.D., n = 16, 4 exper.), y-axis intercept < with F2							

reporter, whereas GR is again an accelerator before the reporter and the CLS.

GREtkLUC Continues to Act at the CLS with Assorted Factors in U2OS Cells—We next asked whether increasing the concentrations of five different factors/cofactors would alter the position of the CLS or the site of GREtkLUC action so that GREtkLUC no longer exerts its dominant effect at the CLS. Again, the approach and type of graphical behavior are identical to those

seen in Figs. 1–3. The specifics for each competition assay are given in Figs. S2–S5 of the supplemental material while Table 1 summarizes the most important graphs and their properties.

The first competitor of GREtkLUC that we examined is GREtkGFP, which encodes the green fluorescent protein (GFP) driven by the same GREtk enhancer/promoter combination as in GREtkLUC. GREtkGFP was selected because it is predicted to be the decelerator that would act closer to the site

Factor and Reporter Mechanisms in Steroid Hormone Action

of GREtkLUC action than any other molecule. As expected, the A_{\max} increases with added GREtkLUC and decreases with GREtkGFP (data not shown). Analysis of the various plots yields one consistent interpretation: GREtkLUC = A = CLS, GREtkGFP = C \leq CLS, and GREtkGFP \leq GREtkLUC (Table 1 and supplemental Figs. S2).

The next factor to be examined is sSMRT. The experiments of Figs. 1 and 2 above indicate that sSMRT is a competitive decelerator (C) before or at the CLS, whereas GREtkLUC is an accelerator at the CLS. We, therefore, asked if the mechanism and site of action of sSMRT and GREtkLUC might change when the two factors are competed against each other, again in U2OS cells. A_{\max} goes down with sSMRT and up with GREtkLUC (data not shown). At the same time, GREtkLUC is still = A = CLS, and sSMRT remains = C \leq CLS (Table 1 and supplemental Figs. S3).

The third factor examined is STAMP. STAMP was originally described as a cofactor that augmented TIF2 coactivator activity both for GR-mediated repression of an exogenous reporter in U2OS cells containing stably transfected rat GR (U2OS.rGR cells) and for GR-regulated induction of exogenous and endogenous genes in CV-1 and U2OS.rGR cells (30). The concentrations of transfected FLAG/STAMP protein in U2OS cells were below the level of detection by Western blotting (data not shown), so we assume that the expression is linear in the range used. Interestingly, in U2OS cells, elevated levels of STAMP decrease the A_{\max} in a manner that is reversed by higher quantities of GREtkLUC (data not shown). At the same time, the competition assay with GREtkLUC and STAMP in the presence of a constant amount of GR reveals that STAMP = C \leq CLS, whereas GREtkLUC = A at the CLS (Table 1 and supplemental Figs. S4). Thus, it appears that the net effect, but not necessarily the kinetically defined mechanism of action, of STAMP with the same exogenous reporter is different in U2OS *versus* CV-1 and U2OS.rGR cells. Notwithstanding, the site and mechanism of action of GREtkLUC remains that of an accelerator at the CLS.

The last two factors studied are two recently described decelerators, NELF-A and a variant of NELF-B,⁶ which are best known as components of the NELF complex (16, 40, 41). Both NELFs reduce the A_{\max} of GR induction as previously reported,⁶ which is countered by higher concentrations of GREtkLUC (data not shown). Western blots indicate that NELF-A, but not NELF-B, expression is linear over the ranges used in the completion assays (data not shown). Therefore, the amounts of NELF-B plasmid were corrected as described under "Experimental Procedures." Although the analysis of most of the data proceeded as above, the graphs of EC_{50}/A_{\max} are not linear, as seen above for sSMRT and STAMP, but rather are nonlinear with an upward curvature (Fig. 4, A and C). The fact that this curvature is eliminated in plots of the square root of EC_{50}/A_{\max} (Fig. 4, B and D) has been described to be a characteristic of a competitive decelerator (previously called a competitive inhibitor but both abbreviated as C) acting at two locations before or at the CLS.⁵ When the position of the lines in the square root plot decrease with higher concentrations of the

second factor as they do here, then the second factor is an accelerator. Therefore, we conclude that in competition assays with GREtkLUC, both NELF-A and NELF-B act as C at two separate sites \leq CLS, whereas GREtkLUC is again A = CLS (Table 1 and supplemental Fig. S5).

GREtkLUC Functions at the CLS in Different Cell Types—The above results suggest that the reporter for GR-regulated transactivation always acts as an accelerator at the CLS with a variety of cofactors in U2OS cells independent of reporter composition (*i.e.* GREtkLUC or MMTVLuc). A more stringent test of this conclusion might be whether the same mechanism and site of action of one reporter is seen in different cell lines. To address this question, we first looked at GREtkLUC actions with different competitors in three other cell lines: green monkey kidney (CV-1) cells, human embryonic kidney 293 cells, and mouse mammary epithelial (1470.2) cells (Table 1 and Figs. S6 and S7 in the supplemental material). In both CV-1 and 293 cells, the A_{\max} of induced luciferase increases with elevated GR and GREtkLUC (data not shown). In both cell lines, GREtkLUC again acts as A = CLS, whereas GR continues to function as A \leq CLS (Table 1 and supplemental Fig. S6).

For the experiments in 1470.2 cells, we examined the competition of GREtkLUC and sSMRT during GR transactivation. In these cells, GREtkLUC elevates, whereas sSMRT depresses the A_{\max} (data not shown). We also find that GREtkLUC = A = CLS, sSMRT = C \leq CLS. Thus the mechanism and site of action of GREtkLUC and sSMRT with GR are the same in 1470.2 and U2OS cells (Table 1 and supplemental Fig. S7).

NCoR Is an Accelerator with GR and GREtkLUC in U2OS Cells—Another frequently studied corepressor, with actions that often mirror SMRT, is NCoR (4). However, there are scattered reports of NCoR appearing to be a coactivator because it causes increased levels of gene transcription (8, 42). We, therefore, competed sSMRT and NCoR directly in U2OS cells. Here we again see NCoR increasing the A_{\max} of induced luciferase, whereas sSMRT causes a decrease (data not shown). Western blots indicated that the amounts of both factors needed to be corrected before graphing due to nonlinear expression (data not shown). As presented in Fig. 5A, the graph of A_{\max}/EC_{50} *versus* NCoR (corrected) is linear with a positive slope. This is diagnostic of an accelerator. Furthermore, the average intersection point in these graphs (x axis = -74 ± 31 ng of NCoR, y axis = -0.04 ± 0.43 , S.D., $n = 3$) is on the x axis and much more negative than the position corresponding to no endogenous NCoR (*i.e.* -8.3 ng of NCoR plasmid). Therefore, this graph is uniquely described by the situation where NCoR = A > CLS and sSMRT = C \leq CLS. These actions limit the possible descriptions of the $1/EC_{50}$ *versus* NCoR plots (Fig. 5B) to two scenarios. If the lines intersect at one point (again, less than no endogenous NCoR), then sSMRT acts at the CLS. If, however, the lines intersect at more than one point, then sSMRT acts before the CLS (see supplemental Table S1 in Dougherty *et al.* (8)). Unfortunately, the data are not precise enough to distinguish between these two possibilities. Therefore, we conclude that NCoR = A > CLS and sSMRT = C \leq CLS. All of the other graphs provide mechanistic interpretations that are consistent with this conclusion (data not shown).

⁶G.-S. Lee, Y. He, E. J. Dougherty, M. Jimenez-Movilla, M. Avella, S. Grullon, D. S. Sharlin, C. Guo, J. A. Blackford, Jr., S. Awasthi, Z. Zhang, S. P. Armstrong, E. C. London, W. Chen, J. Dean, and S. S. Simons, Jr., in preparation.

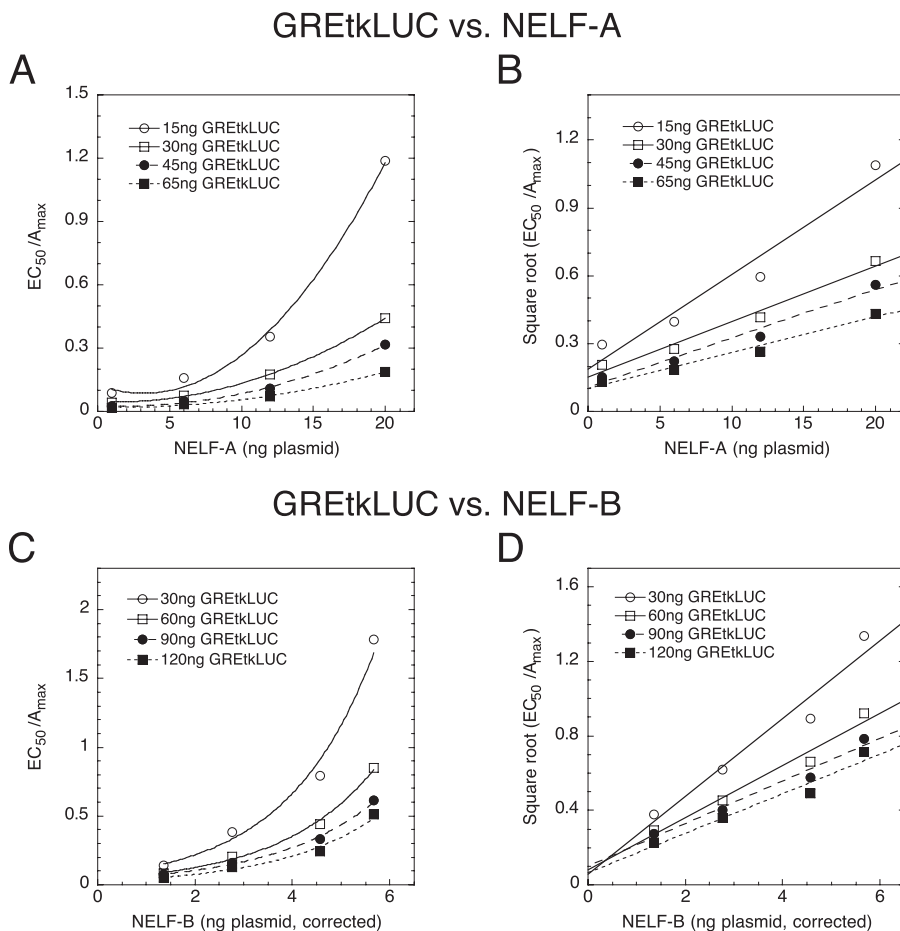


FIGURE 4. Competition of NELFs with GREtkLUC during GR-mediated induction in U2OS cells. Competition assays were conducted and analyzed as in Fig. 1 with the indicated amounts of GREtkLUC and competing factor plasmids plus 1 ng of GR plasmid. *A* and *B*, shown are plots of EC_{50}/A_{max} and the square root of EC_{50}/A_{max} versus NELF-A, respectively, in competition of GREtkLUC versus NELF-A. *C* and *D*, shown plots of EC_{50}/A_{max} and the square root of EC_{50}/A_{max} versus NELF-B, respectively, in competition of GREtkLUC versus NELF-B. Graphs shown are for a single representative experiment (total = 5 for both NELF-A and -B).

NCoR vs. sSMRT

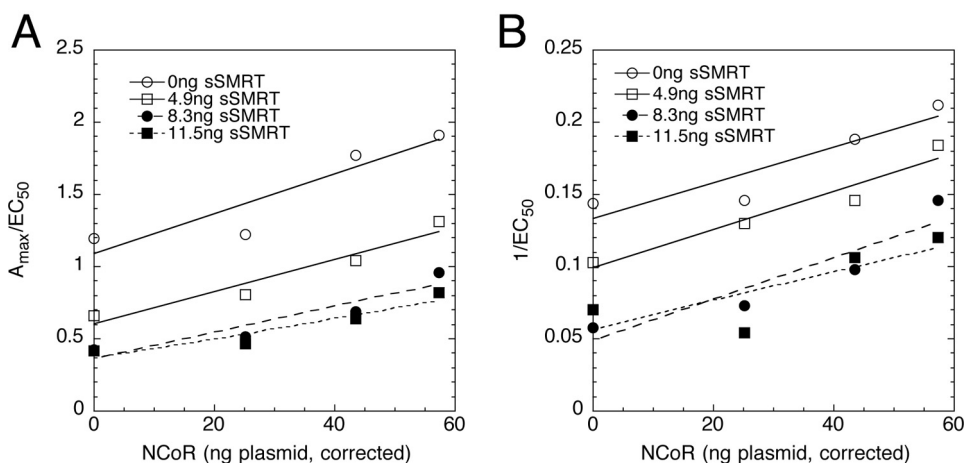


FIGURE 5. Competition of sSMRT and NCoR during GR-mediated induction of GREtkLUC in U2OS cells. Competition assays were conducted and analyzed as in Fig. 1 with the indicated amounts of sSMRT and NCoR plasmids plus 0.2 ng of GR and 100 ng of GREtkLUC plasmids. *A* and *B*, shown are plots of A_{max}/EC_{50} versus NCoR and $1/EC_{50}$ versus NCoR, respectively, in competition of NCoR versus sSMRT. Graphs shown are for a single representative experiment (total = 3).

Mechanism and Site of Factor Action with GR Is Preserved with PR—The classical steroid receptors, bound with their selective ligands, can all activate the common GREtkLUC reporter.

Nonetheless, the qualitative and quantitative responses of the same gene with different receptors are usually not the same (32, 43–46). We, therefore, asked whether the properties of

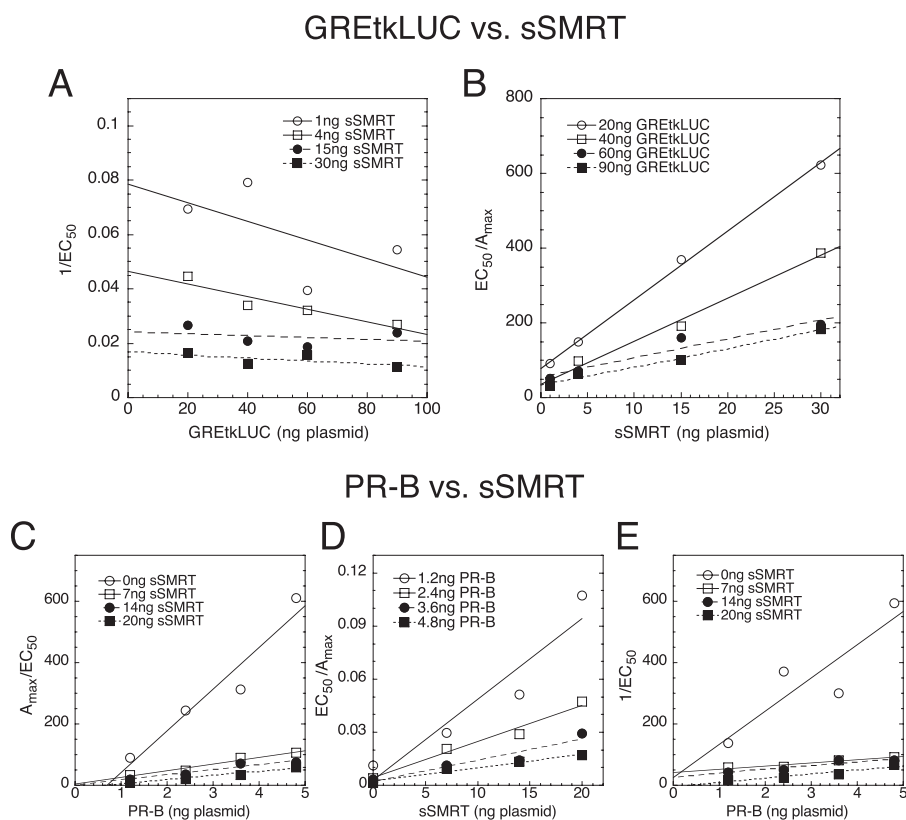


FIGURE 6. **Factor competition during PR-mediated induction of GREtkLUC in 1470.2 cells.** Competition assays were conducted and analyzed as in Fig. 1 with the indicated amounts of plasmids. In these experiments, however, the transfected receptor was PR-B, and the inducing steroid was the synthetic progestin R5020. *A* and *B*, GREtkLUC versus sSMRT competition in the presence of 4 ng PR plasmid is shown. Plots are of $1/EC_{50}$ versus GREtkLUC and EC_{50}/A_{max} versus sSMRT. *C–E*, shown is PR-B versus sSMRT competition in the presence of 100 ng of GREtkLUC. Plots are of A_{max}/EC_{50} versus PR-B, EC_{50}/A_{max} versus sSMRT, and $1/EC_{50}$ versus PR-B, respectively. Graphs shown are for a single representative experiment (total = 4 for both GREtkLUC versus sSMRT and PR-B versus sSMRT).

GREtkLUC and sSMRT action with GR in 1470.2 cells (Table 1) are maintained with PR in the same cells. 1470.2 cells contain endogenous GR but negligible functional amounts of either the large (PR-B) or the small (PR-A) isoform of PR (47). The effects on A_{max} are the same in that GREtkLUC elevates, and sSMRT depresses the A_{max} for PR induction of GREtkLUC in 1470.2 cells (data not shown).

Competition assays of GREtkLUC versus sSMRT under conditions of gene induction by PR-B gave $1/EC_{50}$ versus GREtkLUC plots with zero slope (average = -0.00013 ± 0.00021 , S.D., $n = 16$ lines, 4 experiments) and lower curve positions with higher amounts of sSMRT (Fig. 6A). When combined with the linear EC_{50}/A_{max} versus sSMRT plots (Fig. 6B) and the other graphs (data not shown), the unique conclusion is that GREtkLUC = A = CLS and sSMRT = C \leq CLS. These results suggest that the position and mechanism of action of GREtkLUC is independent of the inducing receptor. Furthermore, the mechanism and position of sSMRT action with PR are the same as those with GR under otherwise identical conditions.

In all of the cases examined above, GR acts as A < CLS (Fig. 2 and Table 1), whereas sSMRT = C \leq CLS (Figs. 1 and 5 and Table 1). To determine whether the activity and placement of PR-B and sSMRT are the same in 1470.2 cells as seen for GR and sSMRT under numerous conditions, we competed PR-B and sSMRT for induction of GREtkLUC in 1470.2 cells. Western blots revealed that the expression of PR-B is linear in the range

used (data not shown) so that no correction is needed. As expected, PR-B augments, and sSMRT diminishes the A_{max} (data not shown). The combination of the A_{max}/EC_{50} versus PR-B lines converging at the origin (Fig. 6C) and linear plots for EC_{50}/A_{max} versus sSMRT (Fig. 6D) limit the possibilities to PR-B = A \leq CLS and sSMRT = C \leq CLS. With these restrictions, the only interpretation of the intersection of the lines in $1/EC_{50}$ versus PR-B at the origin (Fig. 6E) is PR-B = A < CLS and sSMRT = C \leq CLS. These conclusions are identical to those for GR and sSMRT in several cell lines when the same (GREtkLUC) or different (MMTVLuc) reporter is being induced. We, therefore, conclude that the properties of receptor and sSMRT action during reporter induction are independent of the receptor and the cell line and probably also the reporter.

It should be noted that the particular graphical behavior of $1/EC_{50}$ for PR-B versus sSMRT specifies that PR-B acts before sSMRT, which is a conclusion that did not emerge from the above studies with GR and sSMRT. This added information illustrates an important aspect of the competition assay; that is, some combinations of factors yield more detailed information than others.

DISCUSSION

Most models of steroid hormone action are centered on the initial steps where factors and the receptor bind to the pro-

motor region of regulated genes (4, 5). Here we use a new competition assay (6–8) to interrogate all steps, including those that are far downstream of GR binding to the GRE. This method examines pairs of factors and determines both the kinetically defined mechanism of action of each factor and their position in the overall sequence of events relative both to each other and to the CLS. What was unknown at the start of this study was 1) what species acts at the CLS, which is roughly equivalent to the rate-limiting step in enzyme kinetics, and 2) whether the position of the CLS (and thus the molecule(s) acting at the CLS) is constant or changes with the abundance or variety of added factors that modify the A_{\max} and/or EC_{50} . This study presents evidence that CBP, which acts as a platform for numerous associated cofactors, does not act at the CLS. Instead, the reporter gene acts as an accelerator at the CLS in a manner that is independent of the reporter gene (Fig. 1 and Table 1). In addition, the reporter gene continues to act as A = CLS with a variety of accelerators (GR in Fig. 3) and decelerators (GREtkGFP, sSMRT, STAMP, NELF-A, and NELF-B in Table 1 and Fig. 4). Thus the kinetically defined behavior of the reporter is constant regardless of whether the total activity (A_{\max}) goes up or down. This nicely illustrates the independence of the kinetically defined mechanism from the overall activity of the system being examined. Furthermore, the mechanism of the reporter gene is also invariant with changes in cell lines (U2OS, CV-1, 293, and 1470.2 in Table 1) and receptors (GR and PR in Fig. 6 and Table 1). We, therefore, propose that the reporter will always act as an accelerator at the CLS during steroid-regulated gene induction. Furthermore, because our theory of steroid hormone action does not permit two accelerators to act at the same step (6), we conclude that all other accelerators will act either before or after the CLS. Finally, if the reporter always acts at the CLS, it is likely that the position of the CLS does not change. In this case, even when the reporter concentration is not varied, the graphical interpretations of competition assays with two other factors give information about the site of action of each factor relative to the CLS. Thus, the position of the CLS can be used as an invariant marker in the reaction schemes of GR-mediated gene induction, much as Greenwich, England, is used as the universal reference for time around the world.

A summary of the current results that incorporates previous reports of factor actions (6–8, 23) is presented in Fig. 7. This displays the relative ordering of several factors. At the present level of detail, it is interesting that the relative location of factor action appears to be quite constant not only for the reporter (GREtkLUC or MMTVLuc) but also for sSMRT and GR (Table 1). However, more data are required to determine the constancy of how and where each factor acts. As more factors are characterized and added to this scheme, it will be possible not only to expand the ordered sequence of factor action (at least with the gene being examined) but also to construct new competition assays to elucidate the precise sequence of events of factors beyond the current knowledge that they both act before or after the CLS (Fig. 7). Although the theory permits the existence of competitive decelerators after the CLS, it is interesting that no decelerators have been identified so far that act after the CLS.

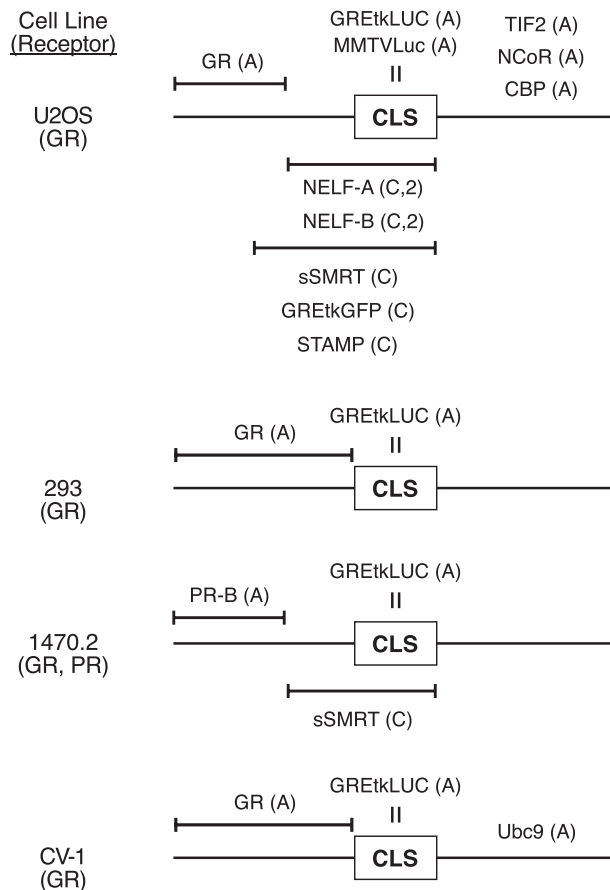


FIGURE 7. Summary of how and where different factors and receptors act during induction of exogenous reporter genes in assorted cell lines. For each cell line, the receptor for which there are data is given in parentheses below the cell name. The horizontal line with the CLS box in the middle represents the unidentified sequence of steps in gene induction that are at the CLS, before the CLS (i.e. to the left of the CLS), or after the CLS (i.e. to the right of the CLS). The range of steps at which each factor has been found to act in the present study relative to the CLS is indicated by the horizontal error bar or by a vertical equal symbol when the precise position is known. For each factor, how the factor acts (accelerator = A, competitive decelerator = C) is given in parentheses after the factor name, with the number 2 designating that competition occurs at two separate steps. The results with TIF2 and Ubc9 are from earlier reports (6, 8). See "Discussion" for additional details.

All of the current experiments were performed with transiently transfected reporter and factors. In the case of the reporter gene, this decision was dictated by the necessity of varying its concentration, something that would be extremely difficult, if not impossible, to do for endogenous genes with the required precision. However, we expect that the present results with exogenous genes extend to many endogenous genes for two reasons. First, GR-regulated genes possess basal level expression and thus do not need extensive chromatin reorganization to permit gene induction. In support of this, studies from Hager and co-workers (48, 49) show that chromatin reorganization in >90% of the GR-regulated genes has already occurred before GR binding to the promoter region. Second, the site and mechanism of action of TIF2 and sSMRT have been found to be the same for both the transiently transfected GREtkLUC reporter and the endogenous IGFBP1 gene (8). Thus, the mechanism and site of action of at least two factors (and probably the CLS) appear to be the same for an exogenous and at least one endogenous gene.

Factor and Reporter Mechanisms in Steroid Hormone Action

The nature of the biochemical reaction in which the reporter participates at the CLS is currently obscure. The reporter is involved in numerous steps in gene induction, such as cofactor binding, formation of the initiation complex, the initiation of transcription, the formation and release of paused polymerase, and elongation by transcribing polymerase being just a few. Given the location of the CLS relative to the actions of the factors so far documented in Fig. 7, we suspect that the CLS is at a relatively early step but after the initial recruitment of cofactors to the promoter region. The nature and location of GREtkGFP action as a competitive decelerator before the CLS is consistent with the GREtkGFP construct competing with GREtkLUC for GR binding. In this case we can conclude that the CLS is downstream of GR binding to the GRE. Future studies are required to elucidate how much further the CLS is downstream of GR binding to the GRE and the biochemical nature of the reaction occurring at the CLS.

One of the reasons for examining the actions of PR in the same competition assays as GR was to pursue our earlier report that sSMRT differentially affects the EC_{50} , but not the A_{max} , of GR versus PR induction of GREtkLUC in 1470.2 cells (32). In particular, sSMRT decreased the A_{max} with both GR and PR. However, sSMRT increased the EC_{50} for PR induction by 3.2-fold while decreasing the EC_{50} for GR induction by a statistically insignificant 1.4-fold. In this study, using very similar amounts of GREtkLUC, sSMRT, and PR plasmids or the same endogenous GR, added sSMRT dramatically increases the EC_{50} for steroid induction of the luciferase reporter by PR (5.39 ± 0.98 -fold, S.E., $n = 8$, $p = 0.0028$, data not shown) compared with a marginal increase in EC_{50} for GR-mediated induction (1.21 ± 0.03 , S.E., $n = 5$, $p = 0.0041$). Thus, sSMRT is again 4.5-fold ($p = 0.0037$) more effective in raising the EC_{50} of gene induction by PR than by GR. The only difference is that, what was initially a weak, statistically not significant reduction (1.4-fold) in the EC_{50} for GR is now an even smaller but significant increase in EC_{50} . We, therefore, conclude that there are no major mechanistic differences between GR and PR with the GREtkLUC and sSMRT in 1470.2 cells, although the ability of sSMRT to increase the EC_{50} is much larger for PR than for GR due to currently unknown reasons.

In summary, we conclude that the gene being induced by GR and PR and probably by most steroid receptors, acts as a kinetically defined accelerator at an invariant position in the sequence of events of steroid-regulated gene transcription under a wide variety of conditions and cell types. Similarly, a smaller selection of reaction conditions suggests that the site of action of GR and of sSMRT is also preserved under many conditions. This leads us to speculate that the site of action of many factors may be preserved as the reaction conditions are varied. In this case, overlapping pairwise assays of those factors that alter A_{max} and/or EC_{50} will be able to construct an ordered sequence of factor action as in Fig. 7 for as many factors as is desired, much as is done in yeast epistasis analysis (50). When applied to endogenous genes for which one desires to regulate the level of expression, such a flow chart of factor action should be helpful in selecting possible factors to regulate because altering the levels or activities of those factors more proximal to the induced gene would be expected to produce fewer side effects

than when targeting more distally located factors. Although the tools for such clinical intervention are not yet available, the recent report that changes in the regulation of expressed gene levels are more important than mutations of selected proteins in the adaptive evolution of the three-spine stickleback fish (51) nicely illustrate the dramatic changes that are possible with altered factor levels. Thus, methods such as the present competition assay should be particularly valuable in systematically identifying proteins that could be pharmaceutical targets for achieving more selective modulation of gene expression.

Acknowledgments—We thank Dan Larson (NCI, National Institutes of Health) and members of the Steroid Hormones Section for constructive criticism of this paper.

REFERENCES

1. Rosenfeld, M. G., and Glass, C. K. (2001) Coregulator codes of transcriptional regulation by nuclear receptors. *J. Biol. Chem.* **276**, 36865–36868
2. Nagy, L., and Schwabe, J. W. (2004) Mechanism of the nuclear receptor molecular switch. *Trends Biochem. Sci.* **29**, 317–324
3. Métivier, R., Reid, G., and Gannon, F. (2006) Transcription in four dimensions. Nuclear receptor-directed initiation of gene expression. *EMBO Rep.* **7**, 161–167
4. Rosenfeld, M. G., Lunyak, V. V., and Glass, C. K. (2006) Sensors and signals. A coactivator/corepressor/epigenetic code for integrating signal-dependent programs of transcriptional response. *Genes Dev.* **20**, 1405–1428
5. Johnson, A. B., and O'Malley, B. W. (2012) Steroid receptor coactivators 1, 2, and 3. Critical regulators of nuclear receptor activity and steroid receptor modulator (SRM)-based cancer therapy. *Mol. Cell. Endocrinol.* **348**, 430–439
6. Ong, K. M., Blackford, J. A., Jr., Kagan, B. L., Simons, S. S., Jr., and Chow, C. C. (2010) A theoretical framework for gene induction and experimental comparisons. *Proc. Natl. Acad. Sci. U.S.A.* **107**, 7107–7112
7. Chow, C. C., Ong, K. M., Dougherty, E. J., and Simons, S. S., Jr. (2011) Inferring mechanisms from dose-response curves. *Methods Enzymol.* **487**, 465–483
8. Dougherty, E. J., Guo, C., Simons, S. S., Jr., and Chow, C. C. (2012) Deducing the temporal order of cofactor function in ligand-regulated gene transcription. Theory and experimental verification. *PLoS ONE* **7**, e30225
9. Fromm, H. J. (1975) *Initial Rate Enzyme Kinetics*, Springer-Verlag, New York
10. Segel, I. H. (1993) *Enzyme Kinetics: Behavior and Analysis of Rapid Equilibrium and Steady-state Enzyme Systems*, Wiley-Interscience, New York
11. Babur, O., Demir, E., Gönen, M., Sander, C., and Dogrusoz, U. (2010) Discovering modulators of gene expression. *Nucleic Acids Res.* **38**, 5648–5656
12. Heemers, H. V., Regan, K. M., Schmidt, L. J., Anderson, S. K., Ballman, K. V., and Tindall, D. J. (2009) Androgen modulation of coregulator expression in prostate cancer cells. *Mol. Endocrinol.* **23**, 572–583
13. Ianculescu, I., Wu, D. Y., Siegmund, K. D., and Stallcup, M. R. (2012) Selective roles for cAMP response element-binding protein-binding protein and p300 protein as coregulators for androgen-regulated gene expression in advanced prostate cancer cells. *J. Biol. Chem.* **287**, 4000–4013
14. Biddie, S. C., John, S., and Hager, G. L. (2010) Genome-wide mechanisms of nuclear receptor action. *Trends Endocrinol. Metab.* **21**, 3–9
15. Rao, N. A., McCalman, M. T., Moulos, P., Francoijs, K. J., Chatziioannou, A., Kolisis, F. N., Alexis, M. N., Mitsiou, D. J., and Stunnenberg, H. G. (2011) Coactivation of GR and NFKB alters the repertoire of their binding sites and target genes. *Genome Res.* **21**, 1404–1416
16. Gilchrist, D. A., Nechaev, S., Lee, C., Ghosh, S. K., Collins, J. B., Li, L., Gilmour, D. S., and Adelman, K. (2008) NELF-mediated stalling of Pol II can enhance gene expression by blocking promoter-proximal nucleosome assembly. *Genes Dev.* **22**, 1921–1933

17. Price, D. H. (2008) Poised polymerases. On your mark . . . get set . . . go! *Mol. Cell* **30**, 7–10
18. Fuda, N. J., Ardehali, M. B., and Lis, J. T. (2009) Defining mechanisms that regulate RNA polymerase II transcription *in vivo*. *Nature* **461**, 186–192
19. Wang, Z., Zang, C., Rosenfeld, J. A., Schones, D. E., Barski, A., Cuddapah, S., Cui, K., Roh, T. Y., Peng, W., Zhang, M. Q., and Zhao, K. (2008) Combinatorial patterns of histone acetylations and methylations in the human genome. *Nat. Genet.* **40**, 897–903
20. Paakinaho, V., Makkonen, H., Jääskeläinen, T., and Palvimo, J. J. (2010) Glucocorticoid receptor activates poised FKBP51 locus through long-distance interactions. *Mol. Endocrinol.* **24**, 511–525
21. Kotekar, A. S., Weissman, J. D., Gegonne, A., Cohen, H., and Singer, D. S. (2008) Histone modifications, but not nucleosomal positioning, correlate with major histocompatibility complex class I promoter activity in different tissues *in vivo*. *Mol. Cell. Biol.* **28**, 7323–7336
22. Stoney Simons, S., Jr. (2003) The importance of being varied in steroid receptor transactivation. *Trends Pharmacol. Sci.* **24**, 253–259
23. Simons, S. S., Jr., and Chow, C. C. (2012) The road less traveled. New views of steroid receptor action from the path of dose-response curves. *Mol. Cell. Endocrinol.* **348**, 373–382
24. Wang, Q., Blackford, J. A., Jr., Song, L. N., Huang, Y., and Cho, S., Simons, S. S., Jr. (2004) Equilibrium interactions of corepressors and coactivators with agonist and antagonist complexes of glucocorticoid receptors. *Mol. Endocrinol.* **18**, 1376–1395
25. Ye, Q., Hu, Y. F., Zhong, H., Nye, A. C., Belmont, A. S., and Li, R. (2001) BRCA1-induced large-scale chromatin unfolding and allele-specific effects of cancer-predisposing mutations. *J. Cell Biol.* **155**, 911–921
26. Szapary, D., Xu, M., and Simons, S. S., Jr. (1996) Induction properties of a transiently transfected glucocorticoid-responsive gene vary with glucocorticoid receptor concentration. *J. Biol. Chem.* **271**, 30576–30582
27. He, Y., Szapary, D., and Simons, S. S., Jr. (2002) Modulation of induction properties of glucocorticoid receptor-agonist and -antagonist complexes by coactivators involves binding to receptors but is independent of ability of coactivators to augment transactivation. *J. Biol. Chem.* **277**, 49256–49266
28. Kaul, S., Blackford, J. A., Jr., Cho, S., and Simons, S. S., Jr. (2002) Ubc9 is a novel modulator of the induction properties of glucocorticoid receptors. *J. Biol. Chem.* **277**, 12541–12549
29. Wang, Q., Anzick, S., Richter, W. F., Meltzer, P., and Simons, S. S., Jr. (2004) Modulation of transcriptional sensitivity of mineralocorticoid and estrogen receptors. *J. Steroid Biochem. Molec. Biol.* **91**, 197–210
30. He, Y., and Simons, S. S., Jr. (2007) STAMP, a novel predicted factor assisting TIF2 actions in glucocorticoid receptor-mediated induction and repression. *Mol. Cell. Biol.* **27**, 1467–1485
31. He, Y., Blackford, J. A., Jr., Kohn, E. C., and Simons, S. S., Jr. (2010) STAMP alters the growth of transformed and ovarian cancer cells. *BMC Cancer* **10**, 128
32. Song, L. N., Huse, B., Rusconi, S., and Simons, S. S., Jr. (2001) Transactivation specificity of glucocorticoid versus progesterone receptors. Role of functionally different interactions of transcription factors with amino- and carboxyl-terminal receptor domains. *J. Biol. Chem.* **276**, 24806–24816
33. Torchia, J., Rose, D. W., Inostroza, J., Kamei, Y., Westin, S., Glass, C. K., and Rosenfeld, M. G. (1997) The transcriptional co-activator p/CIP binds CBP and mediates nuclear-receptor function. *Nature* **387**, 677–684
34. Sarlis, N. J., Bayly, S. F., Szapary, D., and Simons, S. S., Jr. (1999) Quantity of partial agonist activity for antiglucocorticoids complexed with mutant glucocorticoid receptors is constant in two different transactivation assays but not predictable from steroid structure. *J. Steroid Biochem. Molec. Biol.* **68**, 89–102
35. Truss, M., Chalepakis, G., and Beato, M. (1992) *J. Steroid Biochem. Molec. Biol.* **43**, 365–378
36. Tao, Y. G., Xu, Y., Xu, H. E., and Simons, S. S., Jr. (2008) Mutations of glucocorticoid receptor differentially affect AF2 domain activity in a steroid-selective manner to alter the potency and efficacy of gene induction and repression. *Biochemistry* **47**, 7648–7662
37. Lee, G. S., and Simons, S. S., Jr. (2011) Ligand binding domain mutations of the glucocorticoid receptor selectively modify the effects with, but not binding of, cofactors. *Biochemistry* **50**, 356–366
38. Chen, J. D., and Evans, R. M. (1995) A transcriptional co-repressor that interacts with nuclear hormone receptors. *Nature* **377**, 454–457
39. Ordentlich, P., Downes, M., Xie, W., Genin, A., Spinner, N. B., and Evans, R. M. (1999) Unique forms of human and mouse nuclear receptor corepressor SMRT. *Proc. Natl. Acad. Sci. U.S.A.* **96**, 2639–2644
40. Narita, T., Yamaguchi, Y., Yano, K., Sugimoto, S., Chanarat, S., Wada, T., Kim, D. K., Hasegawa, J., Omori, M., Inukai, N., Endoh, M., Yamada, T., and Handa, H. (2003) Human transcription elongation factor NELF. Identification of novel subunits and reconstitution of the functionally active complex. *Mol. Cell. Biol.* **23**, 1863–1873
41. Sun, J., Watkins, G., Blair, A. L., Moskaluk, C., Ghosh, S., Jiang, W. G., and Li, R. (2008) Deregulation of cofactor of BRCA1 expression in breast cancer cells. *J. Cell. Biochem.* **103**, 1798–1807
42. Söderström, M., Vo, A., Heinzel, T., Lavinsky, R. M., Yang, W. M., Seto, E., Peterson, D. A., Rosenfeld, M. G., and Glass, C. K. (1997) Differential effects of nuclear receptor corepressor (N-CoR) expression levels on retinoic acid receptor-mediated repression support the existence of dynamically regulated corepressor complexes. *Mol. Endocrinol.* **11**, 682–692
43. Prior, J. C. (1990) Progesterone as a bone-trophic hormone. *Endocr. Rev.* **11**, 386–398
44. Ziegler, R., and Kasperk, C. (1998) Glucocorticoid-induced osteoporosis. Prevention and treatment. *Steroids* **63**, 344–348
45. Wan, Y., and Nordeen, S. K. (2002) Overlapping but distinct gene regulation profiles by glucocorticoids and progestins in human breast cancer cells. *Mol. Endocrinol.* **16**, 1204–1214
46. Szapary, D., Song, L. N., He, Y., and Simons, S. S., Jr. (2008) Differential modulation of glucocorticoid and progesterone receptor transactivation. *Mol. Cell. Endocrinol.* **283**, 114–126
47. Giannoukos, G., Szapary, D., Smith, C. L., Meeker, J. E., and Simons, S. S., Jr. (2001) New antiprogestins with partial agonist activity. Potential selective progesterone receptor modulators (SPRMs) and probes for receptor- and coregulator-induced changes in progesterone receptor induction properties. *Mol. Endocrinol.* **15**, 255–270
48. Biddie, S. C., John, S., Sabo, P. J., Thurman, R. E., Johnson, T. A., Schiltz, R. L., Miranda, T. B., Sung, M. H., Trump, S., Lightman, S. L., Vinson, C., Stamatoyannopoulos, J. A., and Hager, G. L. (2011) Transcription factor AP1 potentiates chromatin accessibility and glucocorticoid receptor binding. *Mol. Cell* **43**, 145–155
49. John, S., Sabo, P. J., Thurman, R. E., Sung, M. H., Biddie, S. C., Johnson, T. A., Hager, G. L., and Stamatoyannopoulos, J. A. (2011) Chromatin accessibility predetermines glucocorticoid receptor binding patterns. *Nat. Genet.* **43**, 264–268
50. Avery, L., and Wasserman, S. (1992) Ordering gene function. The interpretation of epistasis in regulatory hierarchies. *Trends Genet.* **8**, 312–316
51. Jones, F. C., Grabherr, M. G., Chan, Y. F., Russell, P., Mauceli, E., Johnson, J., Swofford, R., Pirun, M., Zody, M. C., White, S., Birney, E., Searle, S., Schmutz, J., Grimwood, J., Dickson, M. C., Myers, R. M., Miller, C. T., Summers, B. R., Knecht, A. K., Brady, S. D., Zhang, H., Pollen, A. A., Howes, T., Amemiya, C., Broad Institute Genome Sequencing Platform & Whole Genome Assembly Team, Baldwin, J., Bloom, T., Jaffe, D. B., Nicol, R., Wilkinson, J., Lander, E. S., Di Palma, F., Lindblad-Toh, K., and Kingsley, D. M. (2012) The genomic basis of adaptive evolution in threespine sticklebacks. *Nature* **484**, 55–61